Towards precise phenomenology of GPDs

Paweł Sznajder
National Centre for Nuclear Research, Poland

NATIONAL CENTRE FOR NUCLEAR RESEARCH
ŚWIERK

Joint 20th International Workshop on Hadron Structure and Spectroscopy and 5th workshop on Correlations in Partonic and Hadronic Interactions
Yerevan, Armenia, October 2nd, 2024

Deeply Virtual Compton Scattering (DVCS)

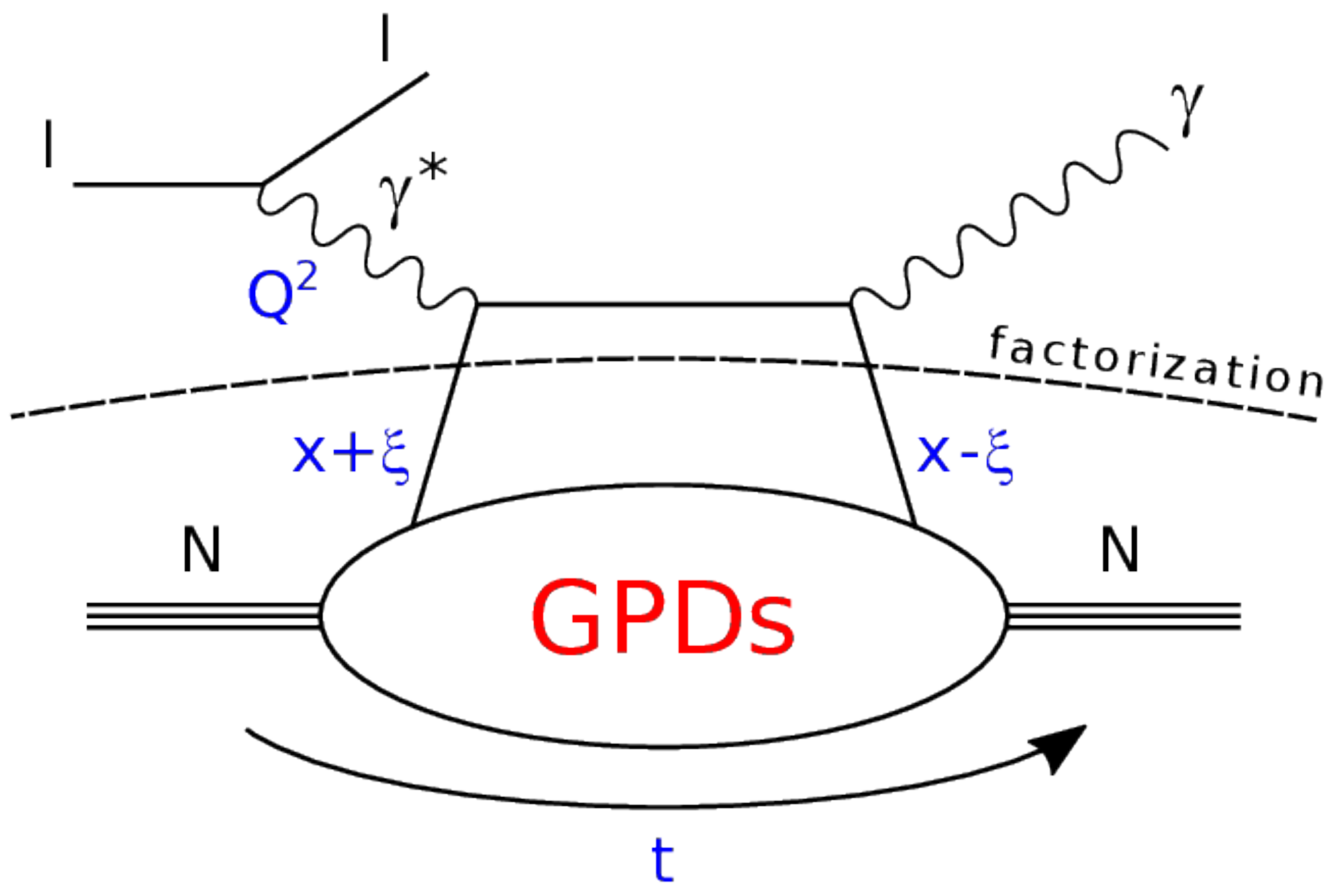

factorisation for $|t|/Q^2 \ll 1$

Chiral-even GPDs:
(helicity of parton conserved)

$H^{q,g}(x,\xi,t)$	$E^{q,g}(x,\xi,t)$	*for sum over parton helicities*
$\widetilde{H}^{q,g}(x,\xi,t)$	$\widetilde{E}^{q,g}(x,\xi,t)$	*for difference over parton helicities*
nucleon helicity conserved	*nucleon helicity changed*	

Introduction

Nucleon tomography:

$$q(x, \mathbf{b}_\perp) = \int \frac{d^2\mathbf{\Delta}_\perp}{(2\pi)^2} e^{-i\mathbf{b}_\perp\cdot\mathbf{\Delta}_\perp} H_q(x, 0, -\mathbf{\Delta}_\perp^2)$$

$$q_X(x, \mathbf{b}_\perp) = q(x, \mathbf{b}_\perp) - \frac{1}{2M}\frac{\partial}{\partial b_y} e_q(x, \mathbf{b}_\perp)$$

$$e_q(x, \mathbf{b}_\perp) = \int \frac{d^2\mathbf{\Delta}_\perp}{(2\pi)^2} e^{-i\mathbf{b}_\perp\cdot\mathbf{\Delta}_\perp} E_q(x, 0, -\mathbf{\Delta}_\perp^2)$$

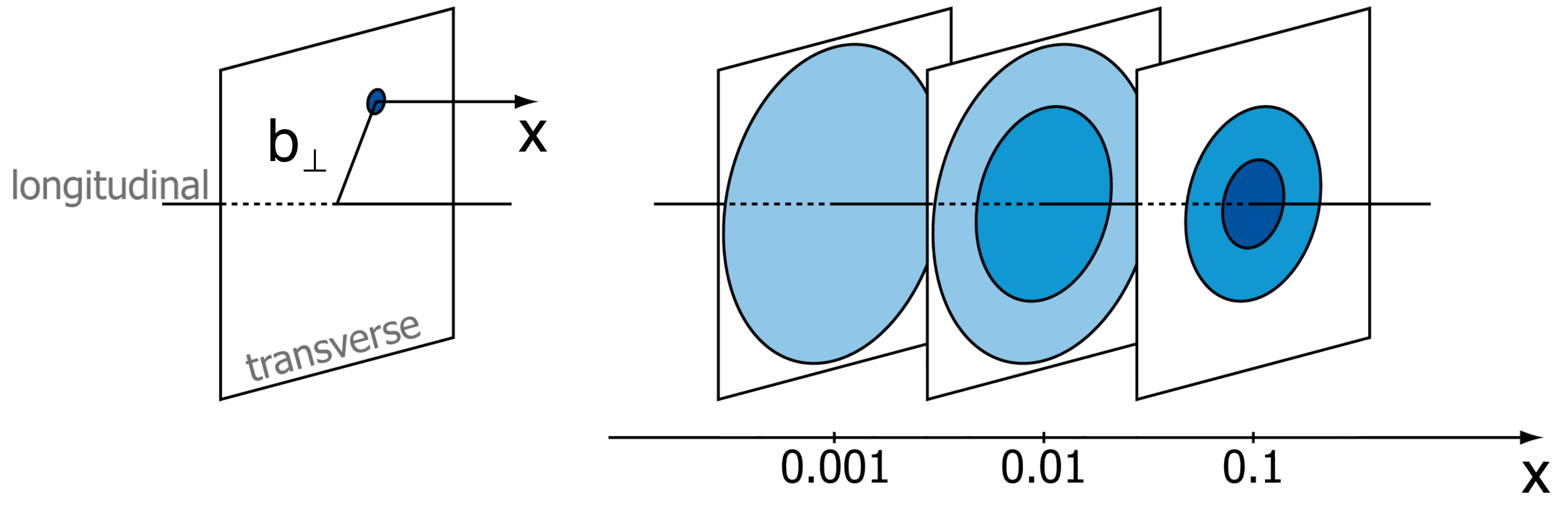

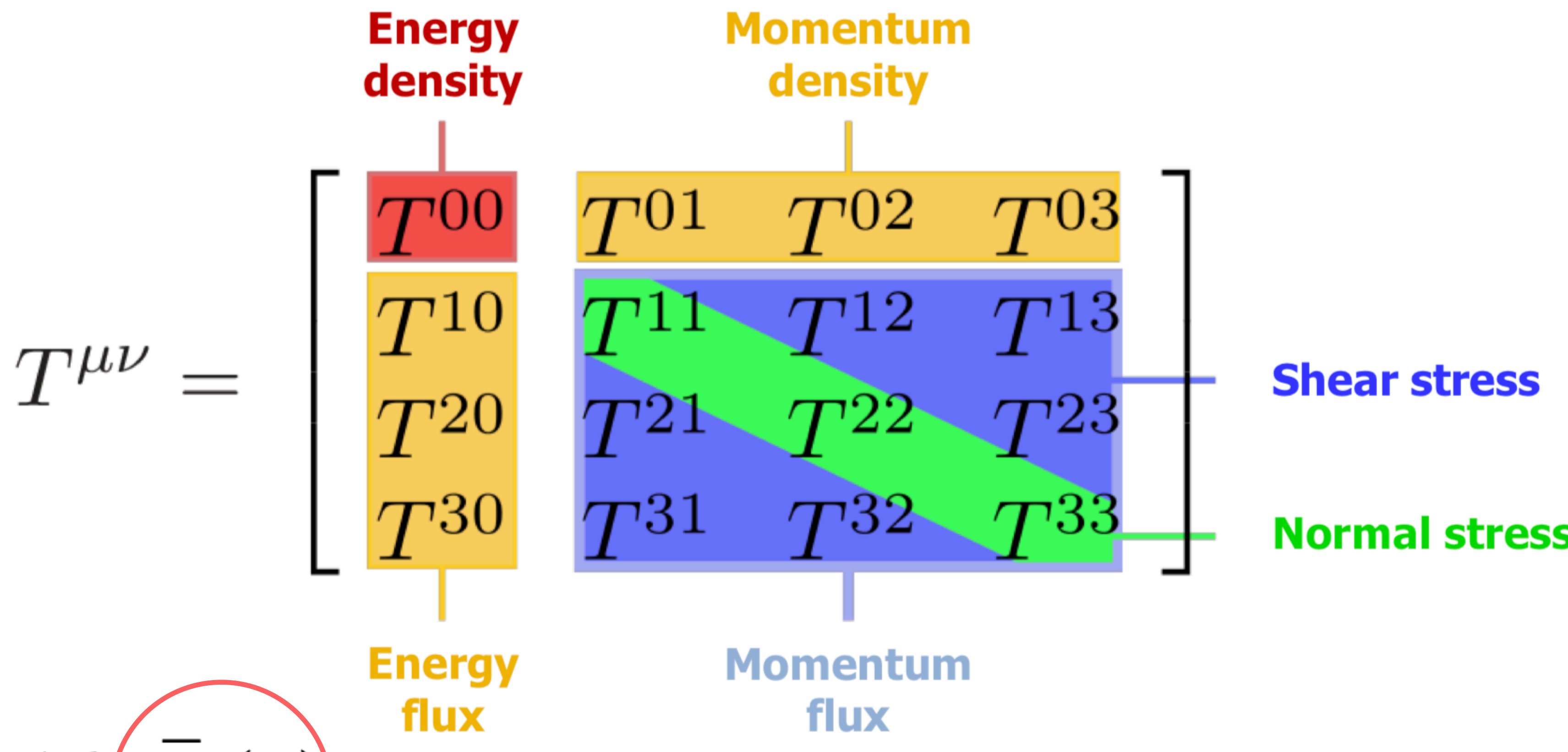

Energy momentum tensor in terms of form factors (OAM and mechanical forces):

$$\langle p', s'|\widehat{T}^{\mu\nu}|p, s\rangle = \bar{u}(p', s')\left[\frac{P^\mu P^\nu}{M} A(t) + \frac{\Delta^\mu\Delta^\nu - \eta^{\mu\nu}\Delta^2}{M} C(t) + M\eta^{\mu\nu}\bar{C}(t) + \frac{P^\mu i\sigma^{\nu\lambda}\Delta_\lambda}{4M}\left[A(t) + B(t) + D(t)\right] + \frac{P^\nu i\sigma^{\mu\lambda}\Delta_\lambda}{4M}\left[A(t) + B(t) - D(t)\right]\right] u(p, s)$$

$$A^q(0) + B^q(0) = \int_{-1}^{1} x\left[H^q(x, \xi, 0) + E^q(x, \xi, 0)\right] = 2J^q$$

Ji’s sum rule

VCS processes provide the most straightforward way to access GPDs (at least from theory side...)

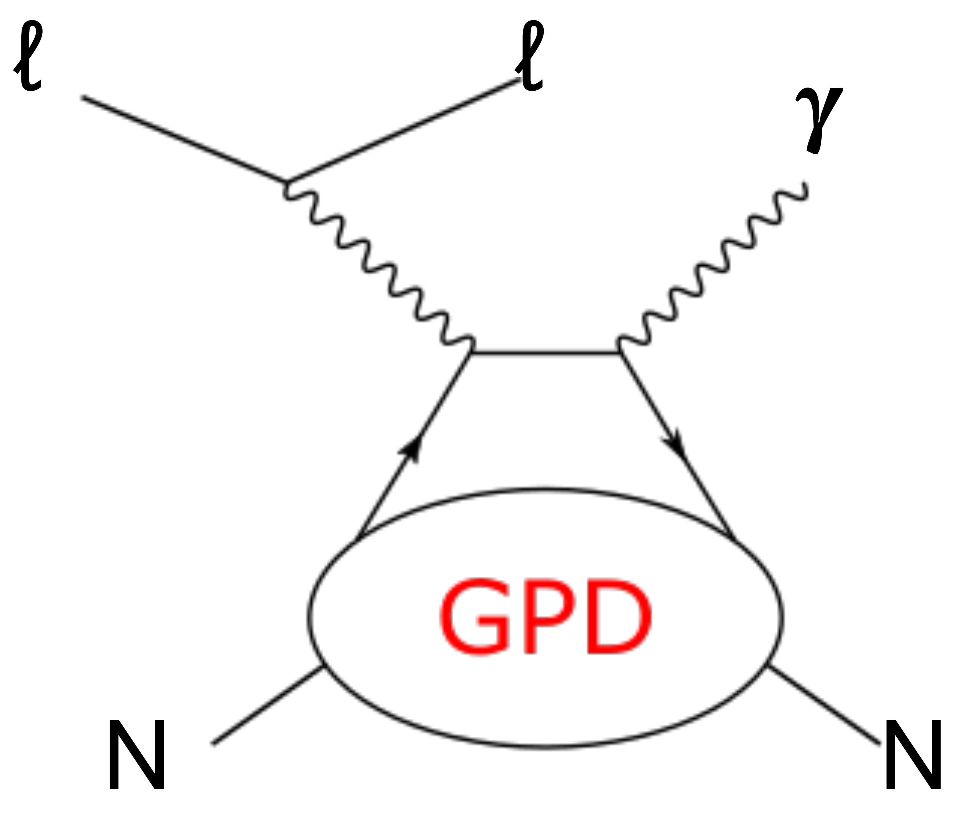

DVCS
Deeply Virtual Compton Scattering

- many measurements, see e.g.: EPJA 52 (2016) 6, 157
- description up to NNLO and twist-4 available PRL 129 (2022) 17, 172001 JHEP 01 (2023) 078

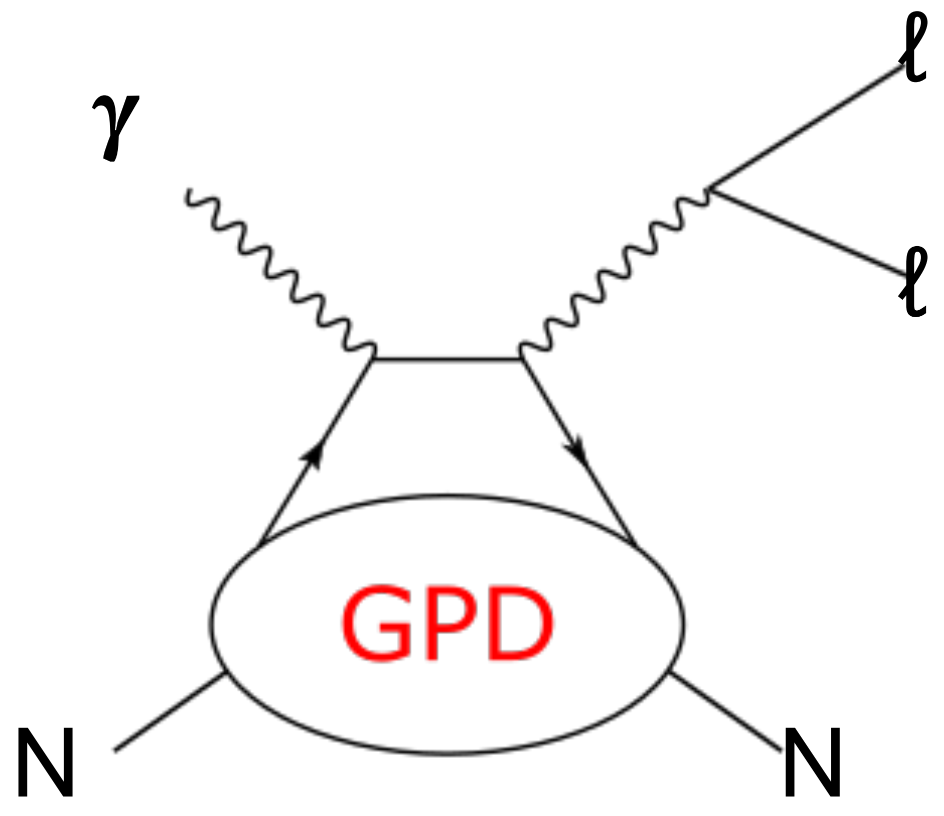

TCS
Timelike Compton Scattering

- first measurement by CLAS PRL 127 (2021) 26, 262501
- description up to NLO and twist-2 available (preliminary tw-4)

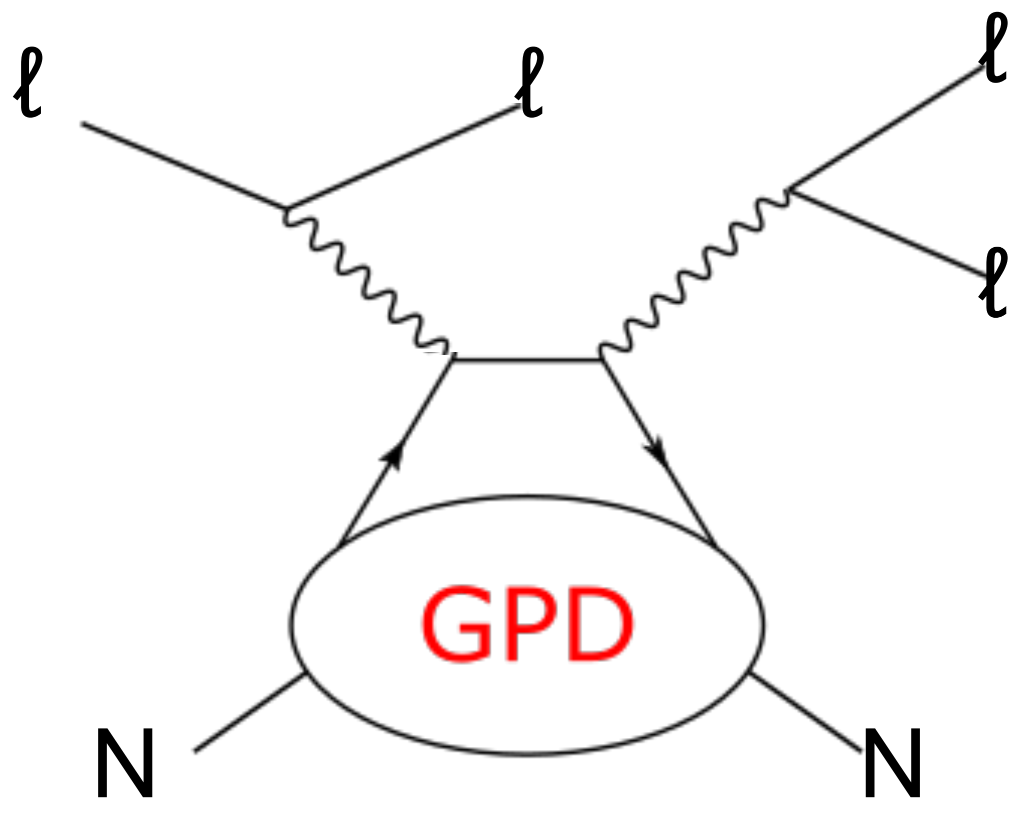

DDVCS
Double Deeply Virtual Compton Scattering

- never measured
- description up to NLO and twist-2 available (preliminary tw-4)

more production channels sensitive to GPDs exist!

Analyses not requiring de-convolution

- probing nucleon tomography at low-xB (see: *JHEP 09 (2013) 093*)

$$d^3\sigma/(dx_{Bj}\,dQ^2\,dt) \propto (\mathrm{Im}\mathcal{H}(\xi,t))^2 \propto \left(\sum_q e_q^2 H^{q(+)}(\xi,\xi,t)\right)^2 \propto \left(\sum_q e_q^2 H^{q(+)}(\xi,0,t)\right)^2$$

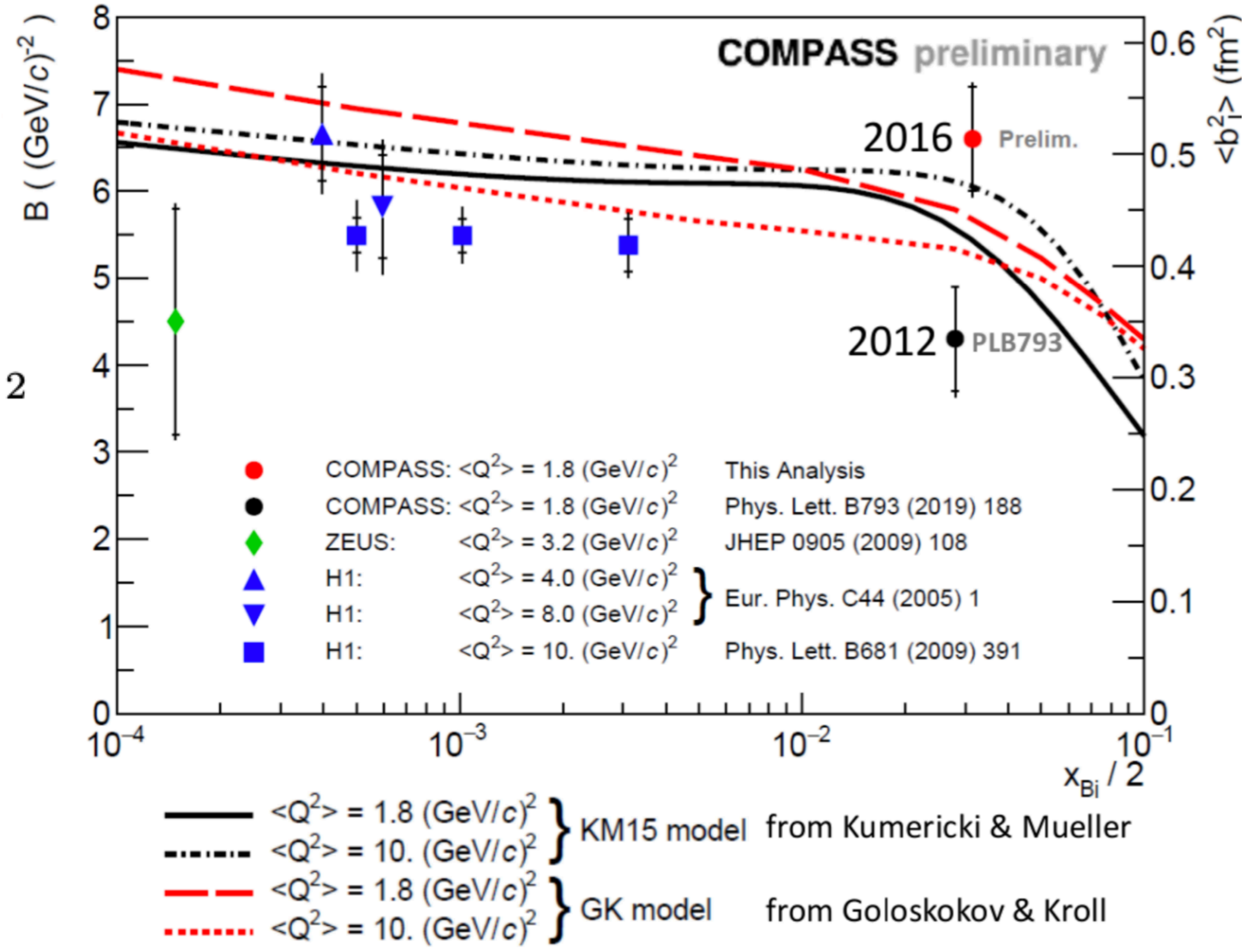

- extraction of D-term
  (see: *Nature 570 (2019) 7759, E1*, *EPJC 81 (2021) 4, 300*)

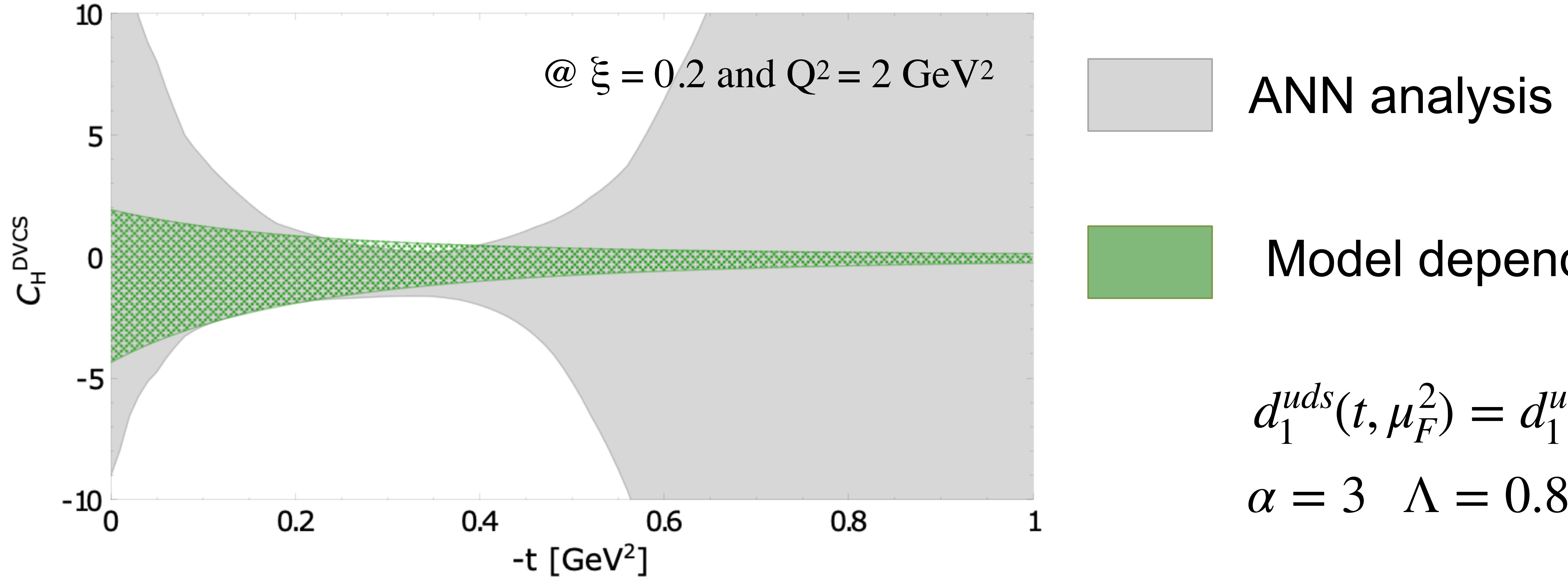

$$d_1^{uds}(t,\mu_F^2) = d_1^{uds}(\mu_F^2)\left(1 - \frac{t}{\Lambda^2}\right)^{-\alpha}$$

$\alpha = 3 \quad \Lambda = 0.8$ GeV

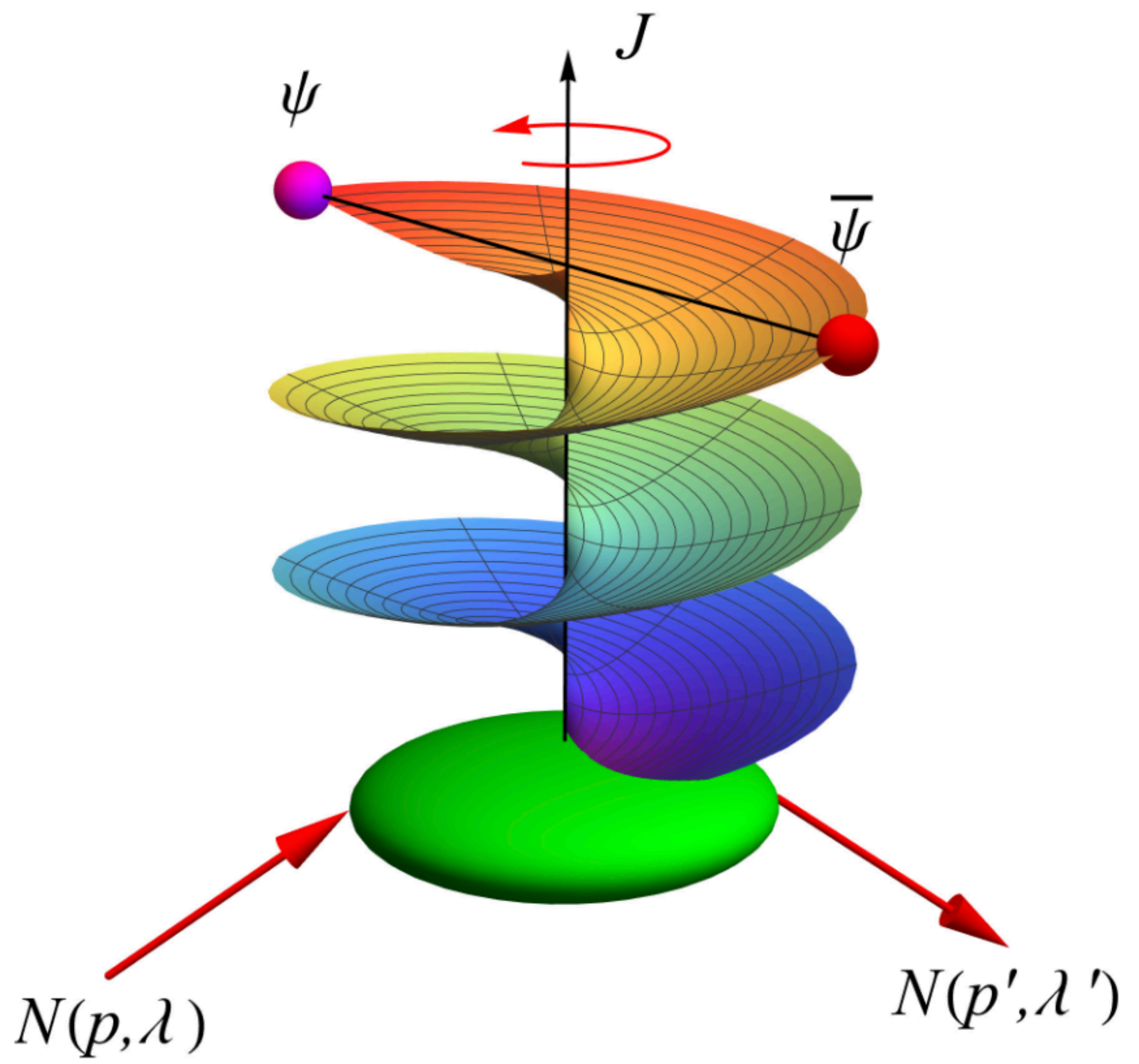

- Froissart-Gribov projections (see: *PRD 109 (2024) 5, 054010*)

Froissart-Gribov projections - spin 0

K. Semenov-Tian-Shansky and P.S.
PRD 109 (2024) 5, 054010

FG projections are obtained by reconstructing cross-channel partial wave expansion amplitudes from the dispersive representation of the amplitude in the direct channel.

In cross-channel: $\gamma^*(q) + \gamma(-q') \to h(p') + \bar{h}(-p)$

Expansion in the cross channel SO(3) partial waves: $\mathcal{H}_+(\cos\theta_t, t) = \sum_{J=0}^{\infty} F_J(t) P_J(\cos\theta_t)$

which gives: $F_J(t) = \frac{2J+1}{2} \int_{-1}^{1} d(\cos\theta_t)\, P_J(\cos\theta_t)\, \mathcal{H}_+(\cos\theta_t, t)$

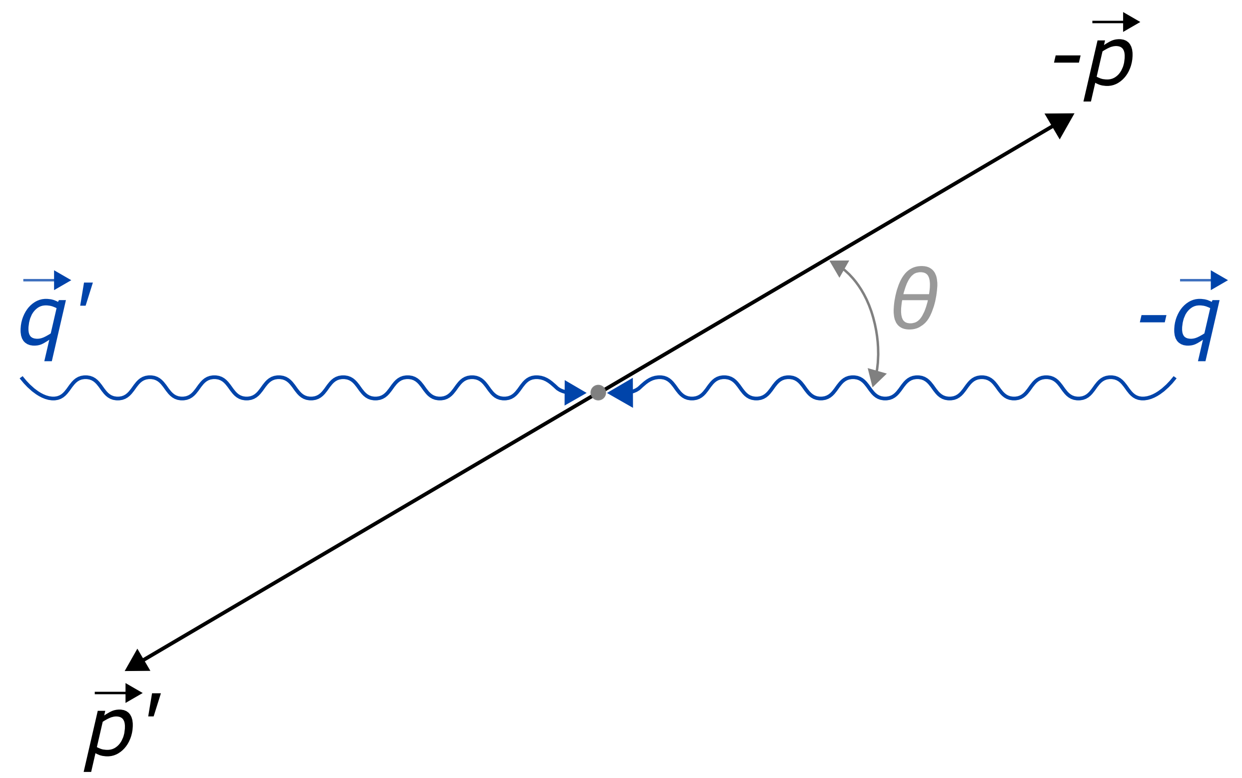

In direct-channel: $\gamma^*(q) + h(p) \to \gamma(q') + h(p')$

Dispersion relation: $\mathrm{Re}\,\mathcal{H}_+(\xi, t) = \mathcal{P}\int_0^1 dx \frac{2x H_+(x,x,t)}{\xi^2 - x^2} + 4D(t)$

where: $\cos\theta_t \to -\frac{1}{\xi\beta} + \mathcal{O}(1/Q^2)$ $\quad \beta = \sqrt{1 - \frac{4m^2}{t}}$

β = 1 in the current analysis (see the publication for discussion of consequences)

Froissart-Gribov projections - spin 0

K. Semenov-Tian-Shansky and P.S.
PRD 109 (2024) 5, 054010

weight functions

Final result:

$$F_{J=0}(t) = 2\int_0^1 dx \left(\frac{\mathcal{Q}_0(1/x)}{x^2} - \frac{1}{x}\right) H_+(x,x,t) + 4D(t)$$

$$F_{J>0}(t) = 2(2J+1)\int_0^1 dx \frac{\mathcal{Q}_J(1/x)}{x^2} H_+(x,x,t)$$

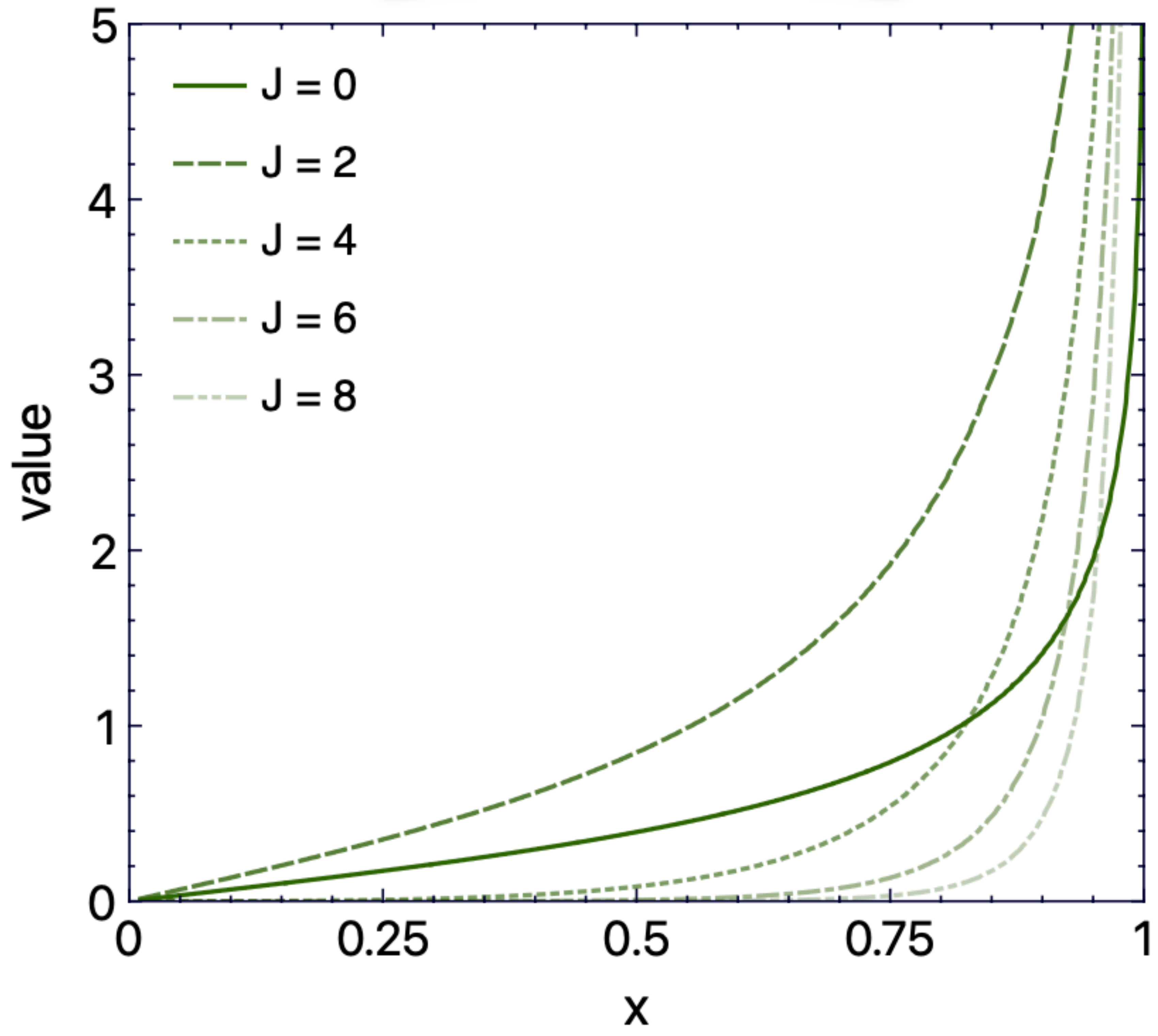

Results for spin-0 target already obtained in
K. Kumericki, D. Mueller, K. Passek-Kumericki, EPJC 58, 193 (2008)

Froissart-Gribov projections - spin ½

NEW!

K. Semenov-Tian-Shansky and P.S.
PRD 109 (2024) 5, 054010

Electric combination:

$$H_{\pm}^{(E)}(x, \cos\theta_t, t) = H_{\pm}(x, \cos\theta_t, t) + \tau E_{\pm}(x, \cos\theta_t, t) \qquad \tau \equiv t/(4m^2)$$

helicities of $p\bar{p}$ *couple to |λ−λ'| = 0*

has to be expanded in $P_J(\cos\theta_t)$ *rotation function*

$$F_{J=0}^{(E)}(t) = 2\int_0^1 dx \left[\frac{\mathcal{Q}_0(1/x)}{x^2} - \frac{1}{x}\right] H_+^{(E)}(x, x, t) + 4(1-\tau)D(t) \qquad F_{J>0}^{(E)}(t) = 2(2J+1)\int_0^1 dx \frac{\mathcal{Q}_0(1/x)}{x^2} H_+^{(E)}(x, x, t)$$

Magnetic combination:

$$H_{\pm}^{(M)}(x, \cos\theta_t, t) = H_{\pm}(x, \cos\theta_t, t) + E_{\pm}(x, \cos\theta_t, t)$$

helicities of $p\bar{p}$ *couple to |λ−λ'| = 1*

has to be expanded in $\sin\theta_t P'_J(\cos\theta_t)/\sqrt{J(J+1)}$ *rotation function*

$$F_J^{(M)}(t) = 2\int_0^1 dx H_+^{(M)}(x, x, t) \frac{2J+1}{J(J+1)} \frac{(-1)}{x} \sqrt{\frac{1}{x^2} - 1}\, \mathcal{Q}_J^1(1/x)$$

Froissart-Gribov projections - spin ½

K. Semenov-Tian-Shansky and P.S.
PRD 109 (2024) 5, 054010

Numerical estimates - electric case:

thin lines and dark bands are estimates for only GPD H

plots for $Q^2 = 2\ GeV^2$

Froissart-Gribov projections - spin ½

K. Semenov-Tian-Shansky and P.S.
PRD 109 (2024) 5, 054010

Numerical estimates - magnetic case:

thin lines and dark bands are estimates for only GPD H

plots for Q^2 = 2 GeV^2

See the publication for more,
in particular for sum rules connecting FG projections with Mellin moments

Double DVCS

K. Deja, V. Martínez-Fernández,
B. Pire, PS, J. Wagner
Phys. Rev. D 107 (2023) 9, 094035

- The process allows to directly probe GPDs outside x=ξ line, but is much more challenging experimentally

$$\xi = \frac{Q^2 + Q'^2}{2Q^2/x_B - Q^2 - Q'^2}$$

$$(\mathcal{H}, \mathcal{E})(\rho, \xi, t) = \sum_{f=\{u,d,s\}} \int_{-1}^{1} dx\, C_f^{(-)}(x, \rho)(H_f, E_f)(x, \xi, t)$$

$$\rho = \xi \frac{Q^2 - Q'^2}{Q^2 + Q'^2}$$

$$C_f^{(\pm)}(x, \rho) \overset{LO}{=} \left(\frac{e_f}{e}\right)^2 \left(\frac{1}{\rho - x - i0} \pm \frac{1}{\rho + x - i0}\right)$$

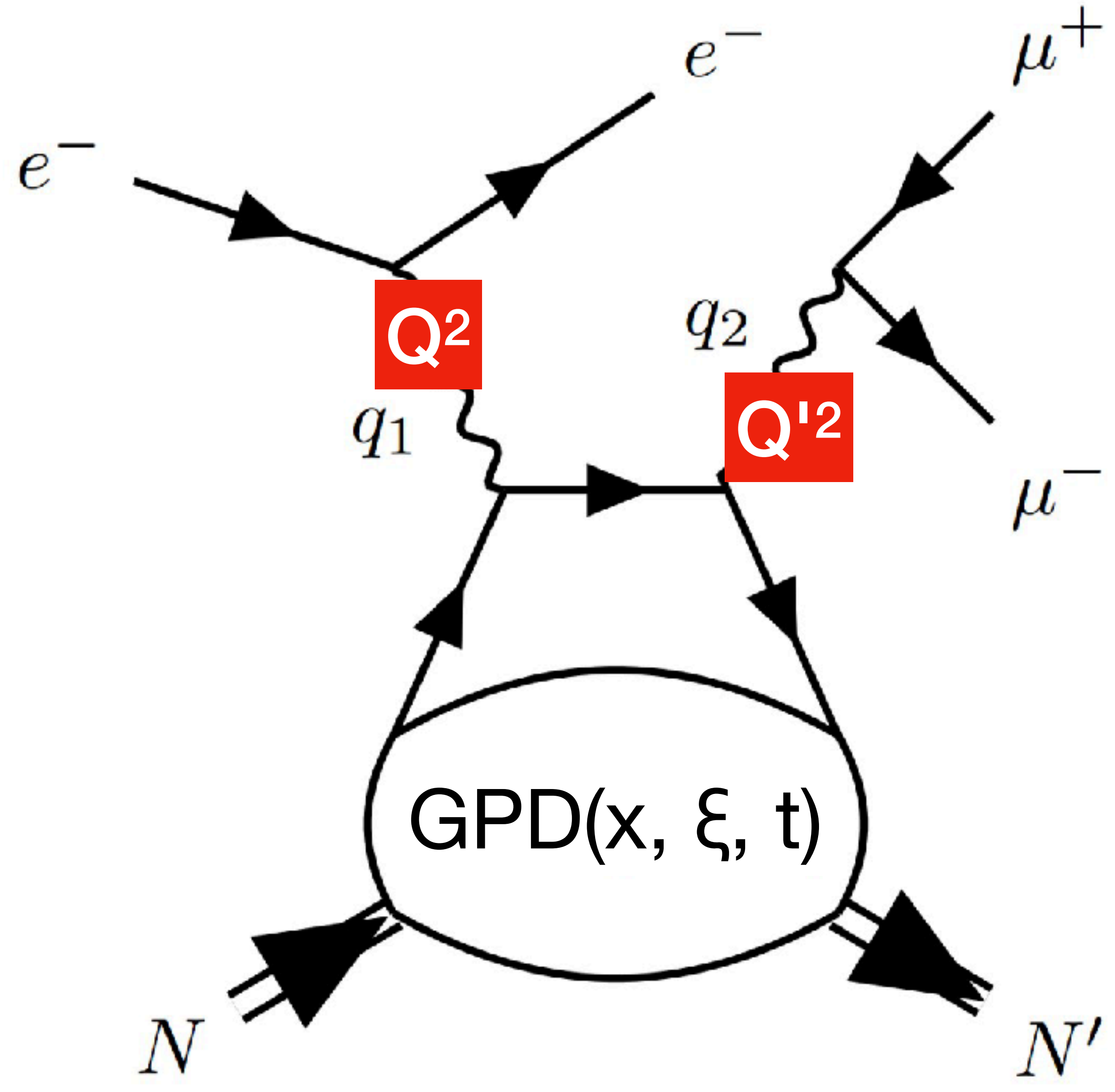

- We revisit DDVCS phenomenology in view of new experiments, including reevaluation of DDVCS and BH cross-sections with Kleiss-Stirling spinor techniques

- Obtained results are available in PARTONS and EpIC MC generator

Double DVCS

K. Deja, V. Martínez-Fernández, B. Pire, PS, J. Wagner Phys. Rev. D 107 (2023) 9, 094035

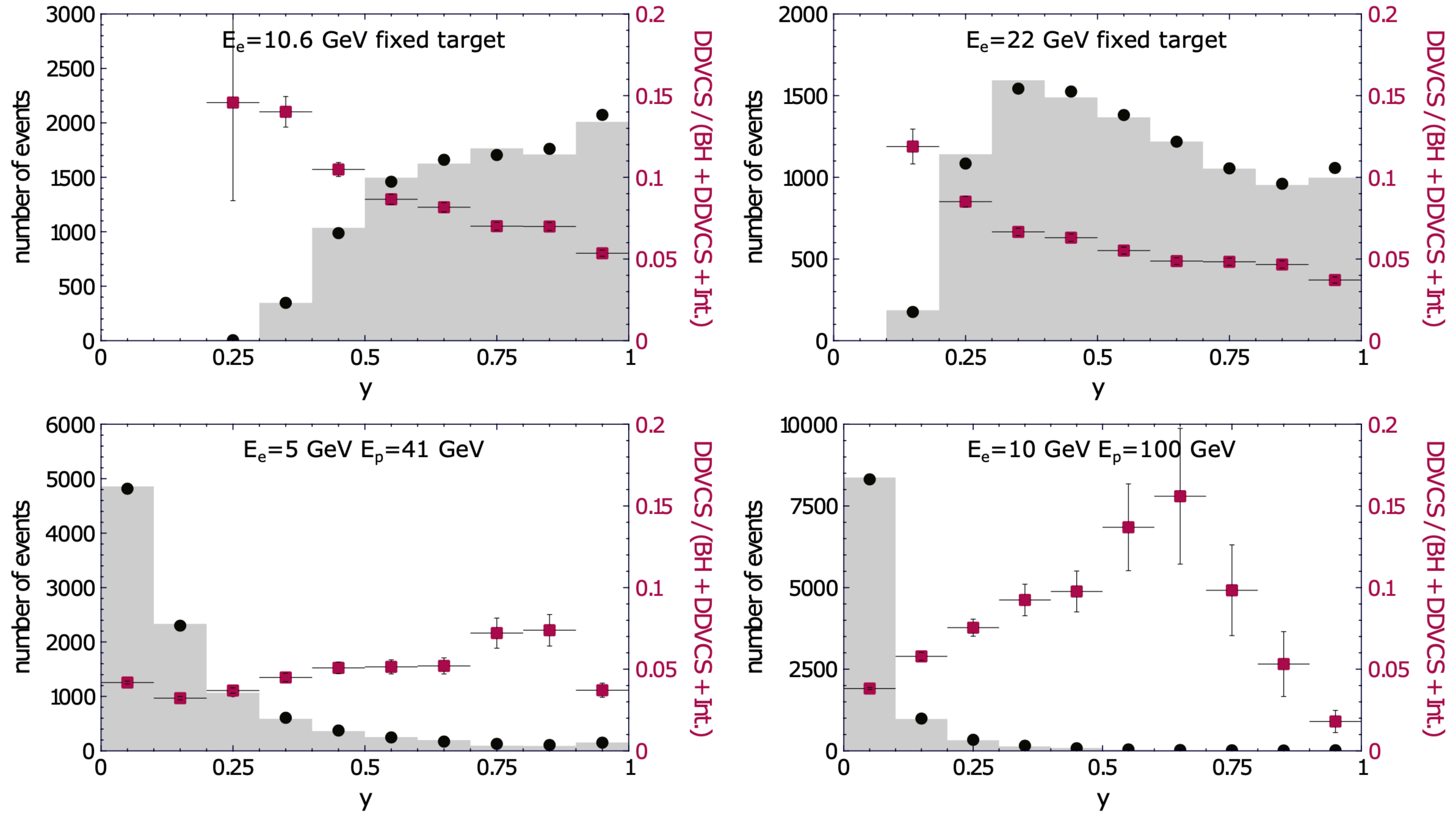

EpIC MC

● integrated cross-section

■ pure DDVCS contribution

Kinematic cuts:

- 0.15 GeV^2 < Q^2 < 5 GeV^2
- 2.25 GeV^2 < Q'^2 < 9 GeV^2
- 0.1 GeV^2 < t < 0.8 GeV^2 (JLab)
- 0.05 GeV^2 < t < 1 GeV^2 (EIC)
- 0.1 < φ, φ_l < 2π − 0.1
- π/4 < θ_l < 3π/4
- 0.1 < y < 1 (JLab)
- 0.05 < y < 1 (EIC)

Experiment	Beam energies [GeV]	Range of $\|t\|$ [GeV^2]	$\sigma\|_{0<y<1}$ [pb]	$\mathcal{L}^{10k}\|_{0<y<1}$ [fb^{-1}]	$y_{\min}$	$\sigma\|_{y_{\min}<y<1}/\sigma\|_{0<y<1}$
JLab12	$E_e = 10.6,\ E_p = M$	$(0.1, 0.8)$	0.14	70	0.1	1
JLab2+	$E_e = 22,\ E_p = M$	$(0.1, 0.8)$	0.46	22	0.1	1
EIC	$E_e = 5,\ E_p = 41$	$(0.05, 1)$	3.9	2.6	0.05	0.73
EIC	$E_e = 10,\ E_p = 100$	$(0.05, 1)$	4.7	2.1	0.05	0.32

Predictions for EIcC will be released soon!

Double DVCS

K. Deja, V. Martínez-Fernández, B. Pire, PS, J. Wagner
Phys. Rev. D 107 (2023) 9, 094035

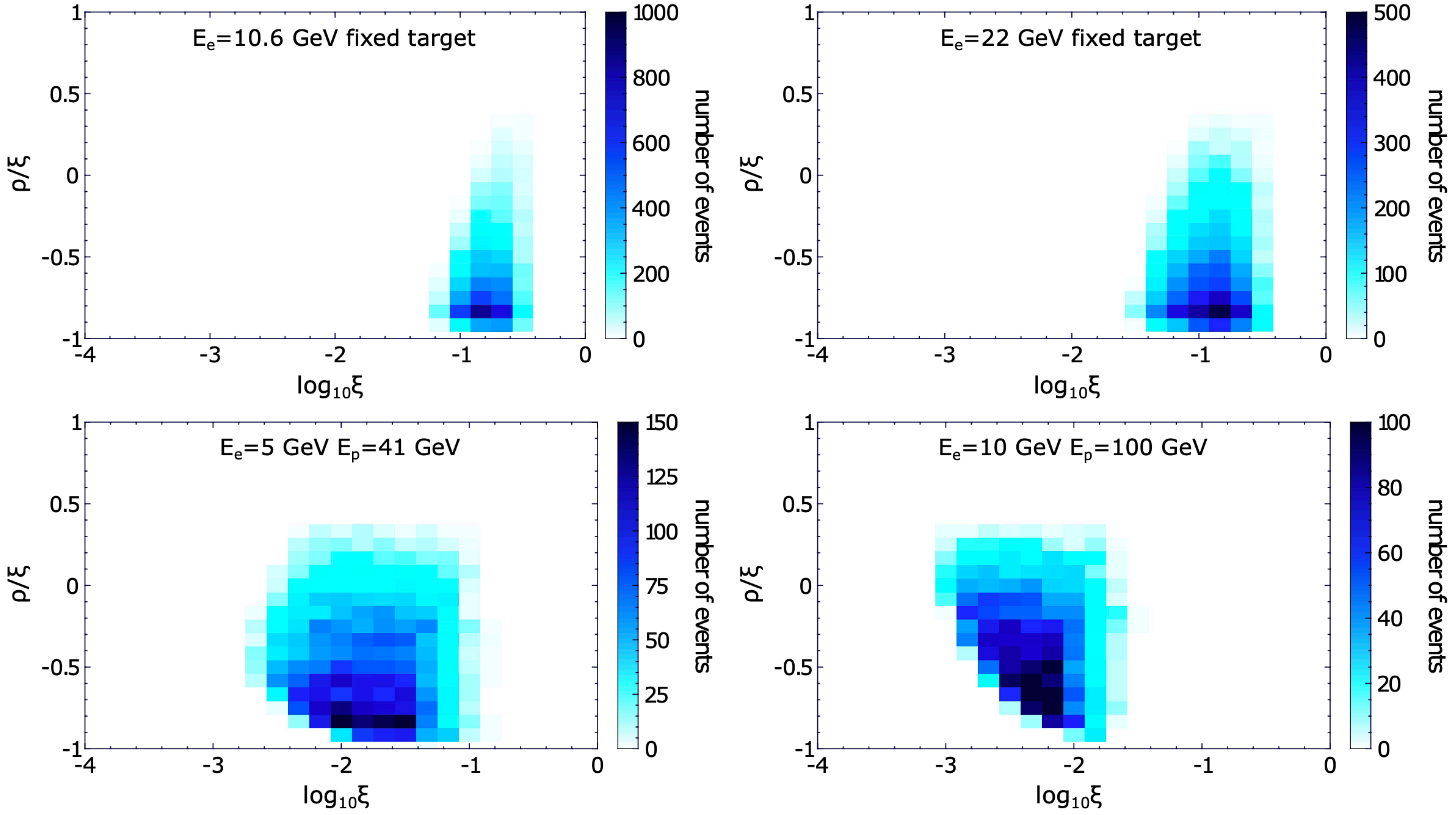

Kinematic cuts:

- 0.15 GeV^2 < Q^2 < 5 GeV^2
- 2.25 GeV^2 < Q'^2 < 9 GeV^2
- 0.1 GeV^2 < t < 0.8 GeV^2 (JLab)
- 0.05 GeV^2 < t < 1 GeV^2 (EIC)
- 0.1 < φ, φ_l < 2π − 0.1
- π/4 < θ_l < 3π/4
- 0.1 < y < 1 (JLab)
- 0.05 < y < 1 (EIC)

Predictions for EIcC will be released soon!

Double DVCS at twist-4

V. Martínez-Fernández,
B. Pire, PS, J. Wagner
preliminary

- Starting point: OPE + CFT (Braun-Ji-Manashov result)
  (see: JHEP 03 (2021) 051 and JHEP 01 (2023) 078)

$$T^{\mu\nu} = i\int d^4z\, e^{iq'z}\langle p'|\mathcal{T}\{j^\mu(z)j^\nu(0)\}|p\rangle$$

$$= \frac{1}{i\pi^2} i\int d^4z\, e^{iq'z}\left\{\frac{1}{(-z^2+i0)^2}\left[g^{\mu\nu}\mathcal{O}(1,0) - z^\mu\partial^\nu\int_0^1 du\,\mathcal{O}(\bar{u},0) - z^\nu(\partial^\mu - i\Delta^\mu)\int_0^1 dv\,\mathcal{O}(1,v)\right]\right. + \ldots$$

where $\mathcal{O}, \mathcal{O}_1, \mathcal{O}_2$ are matrix elements $\langle p'|\mathcal{O}|p\rangle, \langle p'|\mathcal{O}_1|p\rangle, \langle p'|\mathcal{O}_2|p\rangle$ containing information about GPDs

- For spin-0 target:

$$T^{\mu\nu} = \mathcal{A}^{00}\frac{-i}{QQ'R^2}\left[(qq')(Q'^2q^\mu q^\nu - Q^2q'^\mu q'^\nu) + Q^2Q'^2q^\mu q'^\nu - (qq')^2q'^\mu q^\nu\right]$$

$$+ \mathcal{A}^{+0}\frac{i\sqrt{2}}{R|\bar{p}_\perp|}\left[Q'q^\mu - \frac{qq'}{Q'}q'^\mu\right]\bar{p}_\perp^\nu + \mathcal{A}^{0+}\frac{\sqrt{2}}{R|\bar{p}_\perp|}\bar{p}_\perp^\mu\left[\frac{qq'}{Q}q^\nu + Qq'^\nu\right]$$

$$+ \mathcal{A}^{+-}\frac{1}{|\bar{p}_\perp|^2}\left[\bar{p}_\perp^\mu\bar{p}_\perp^\nu - \tilde{\bar{p}}_\perp^\mu\tilde{\bar{p}}_\perp^\nu\right] + \mathcal{A}^{++}g_\perp^{\mu\nu},$$

$$R = \sqrt{(qq')^2 + Q^2Q'^2}$$

Double DVCS at twist-4

V. Martínez-Fernández, B. Pire, PS, J. Wagner
preliminary

- Numerical estimate (only for A++):

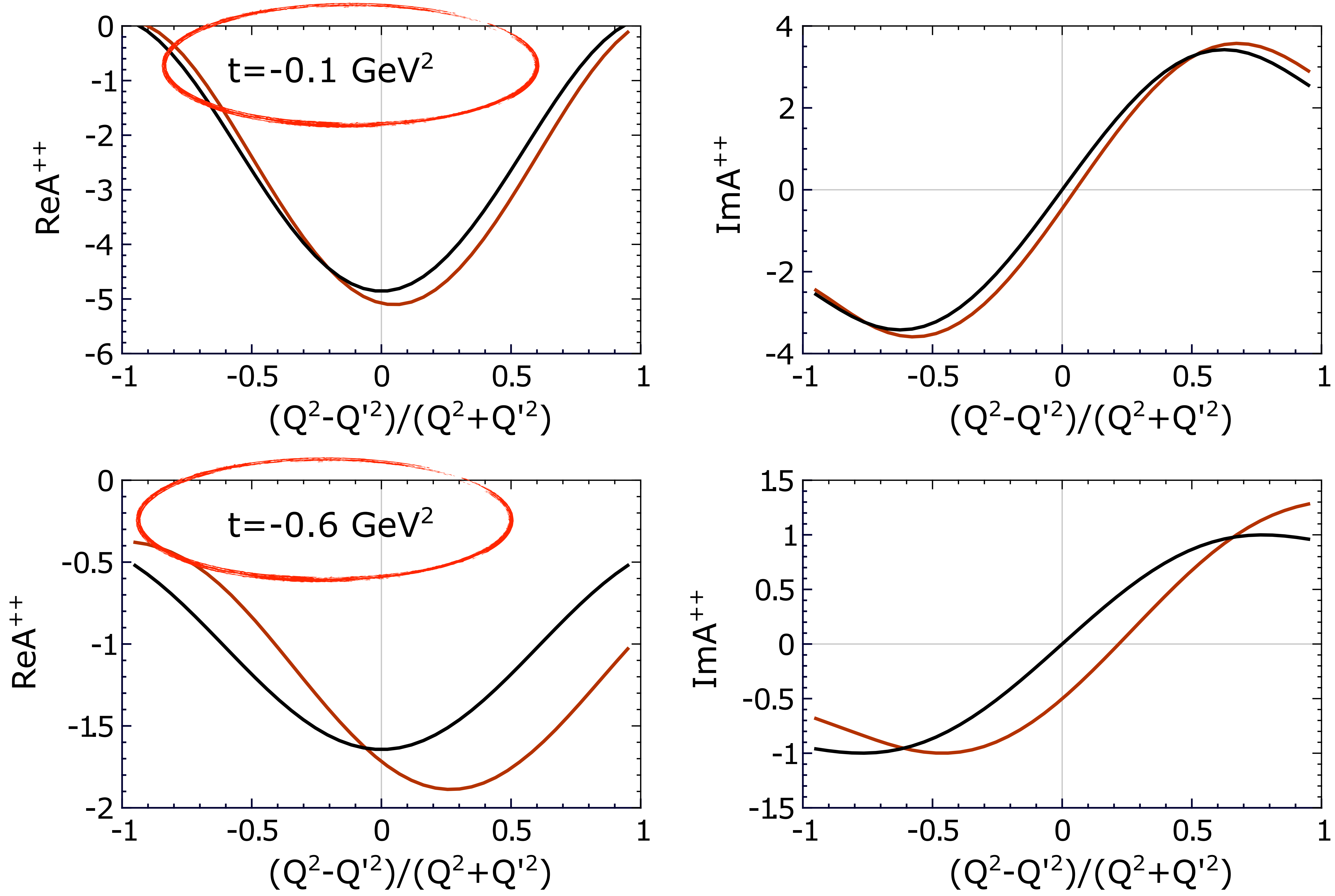

DVCS: $Q'^2 = 0$

TCS: $Q^2 = 0$

twist-2
up to twist-4

$\xi = 0.2$

$\mu^2 = 1.9\ \text{GeV}^2$

GPD model from:
PRD 105, 094012 (2022)

Note:

- at LT: $A^{++}_{\text{DVCS}} = (A^{++}_{\text{TCS}})^*$
- does not hold with HT corrections

Dictionary

- GPDs in Ioffe time:

$$\hat{H}(\nu, \xi, t) = \int_{-1}^{1} \mathrm{d}x\, e^{ix\nu} H(x, \xi, t)$$

- Single and non-singlet combinations of GPDs

$$H^{(+)}(x, \xi, t) = H(x, \xi, t) - H(-x, \xi, t)$$

$$H^{(-)}(x, \xi, t) = H(x, \xi, t) + H(-x, \xi, t)$$

- Therefore:

$$\mathrm{Re}\hat{H}(\nu, \xi, t) = \int_{0}^{1} \mathrm{d}x\ \cos(x\nu) H^{(-)}(x, \xi, t)$$

$$\mathrm{Im}\hat{H}(\nu, \xi, t) = \int_{0}^{1} \mathrm{d}x\ \sin(x\nu) H^{(+)}(x, \xi, t)$$

- At ξ=0:

$$H^{(+)}(x,0,t) = \mathrm{sgn}(x)\big(H_{\mathrm{val}}(|x|,0,t) + 2H_{\mathrm{sea}}(|x|,0,t)\big)$$

$$H^{(-)}(x,0,t) = H_{\mathrm{val}}(|x|,0,t)$$

Lattice-QCD data - comparison with models for GPD H at ξ=0

K. Cichy, M. Constantinou, PS, J. Wagner
arXiv: hep-ph/2409.17955

t=0 (PDF)

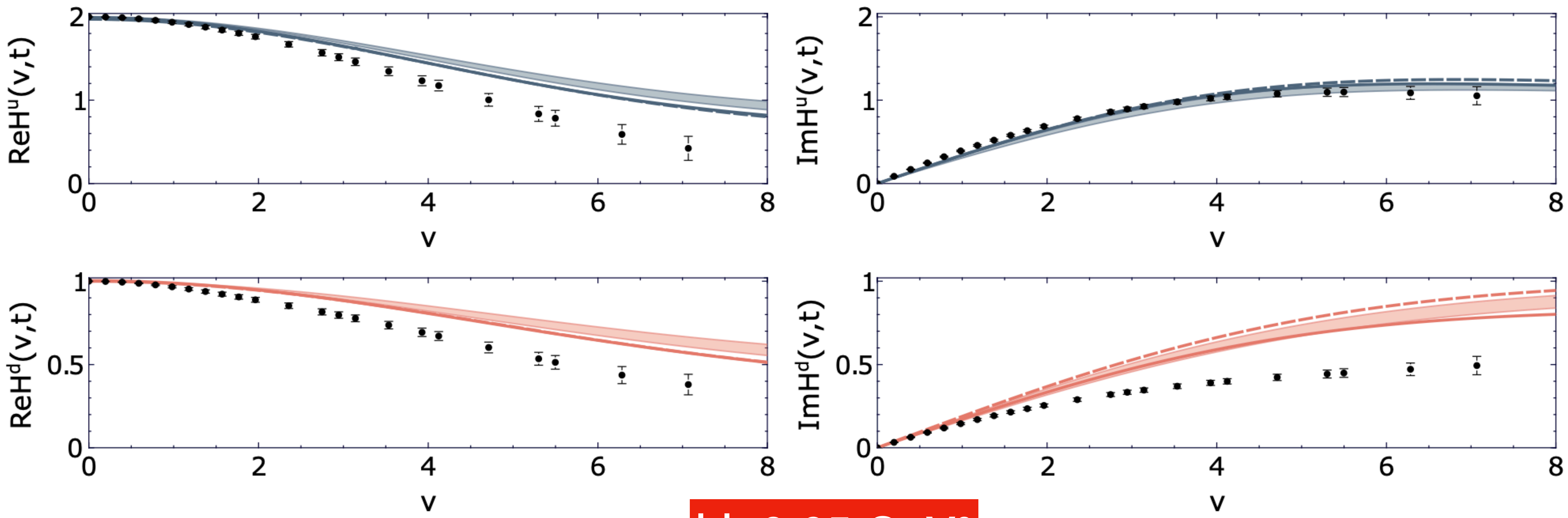

ν=0 (elastic FF)
(imaginary part vanishes)

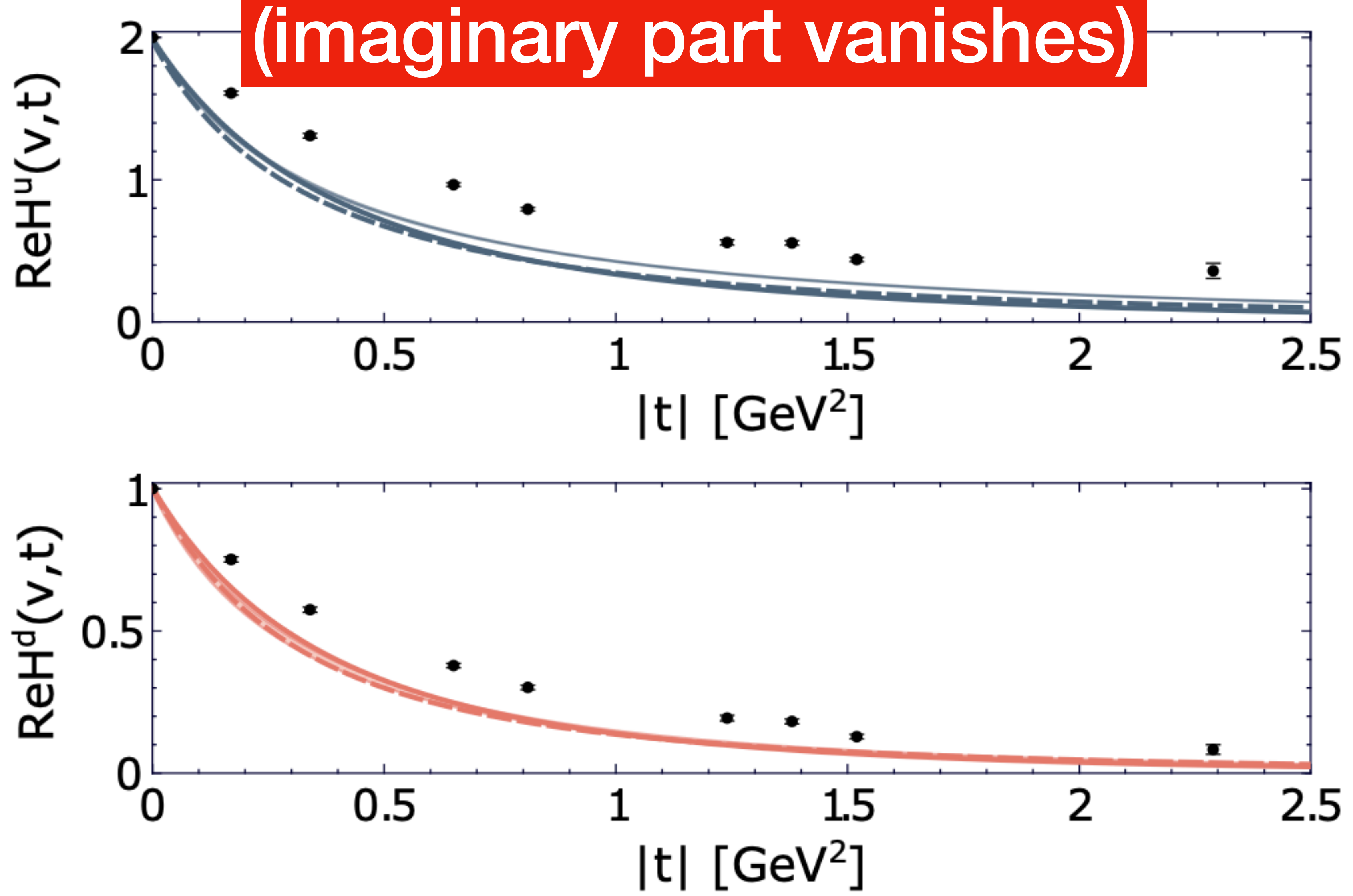

$|t|$=0.65 GeV^2

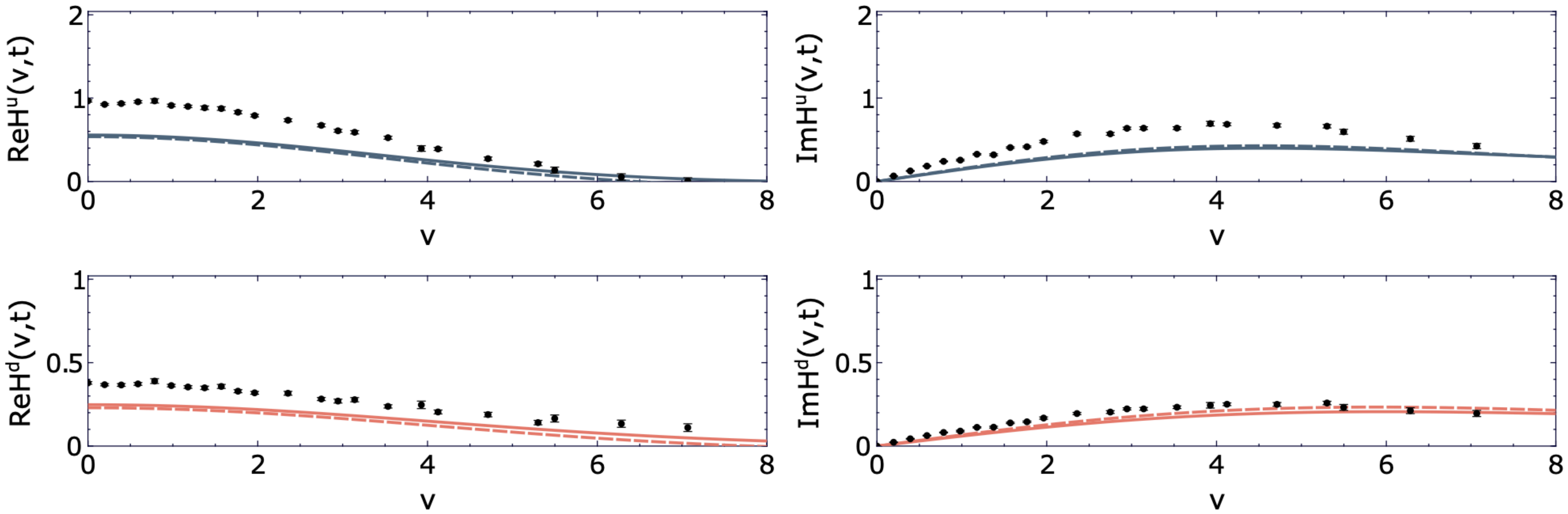

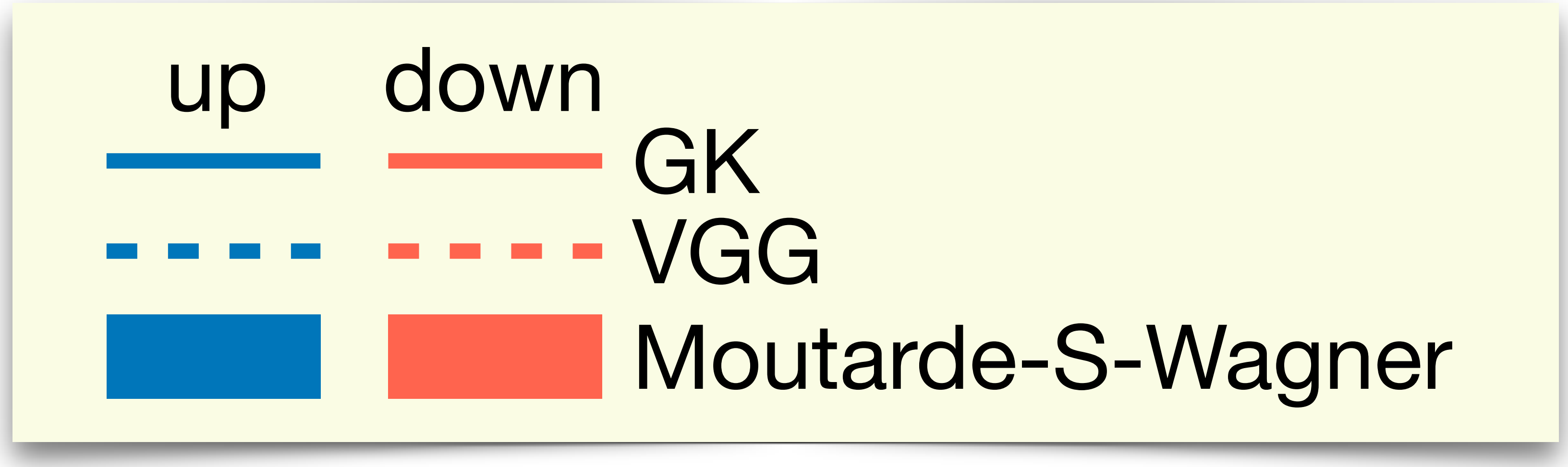

Lattice-QCD data - comparison with models for GPD H at ξ=0

K. Cichy, M. Constantinou, PS, J. Wagner
arXiv: hep-ph/2409.17955

|t|=0.65 GeV² ("original" lattice-QCD results)

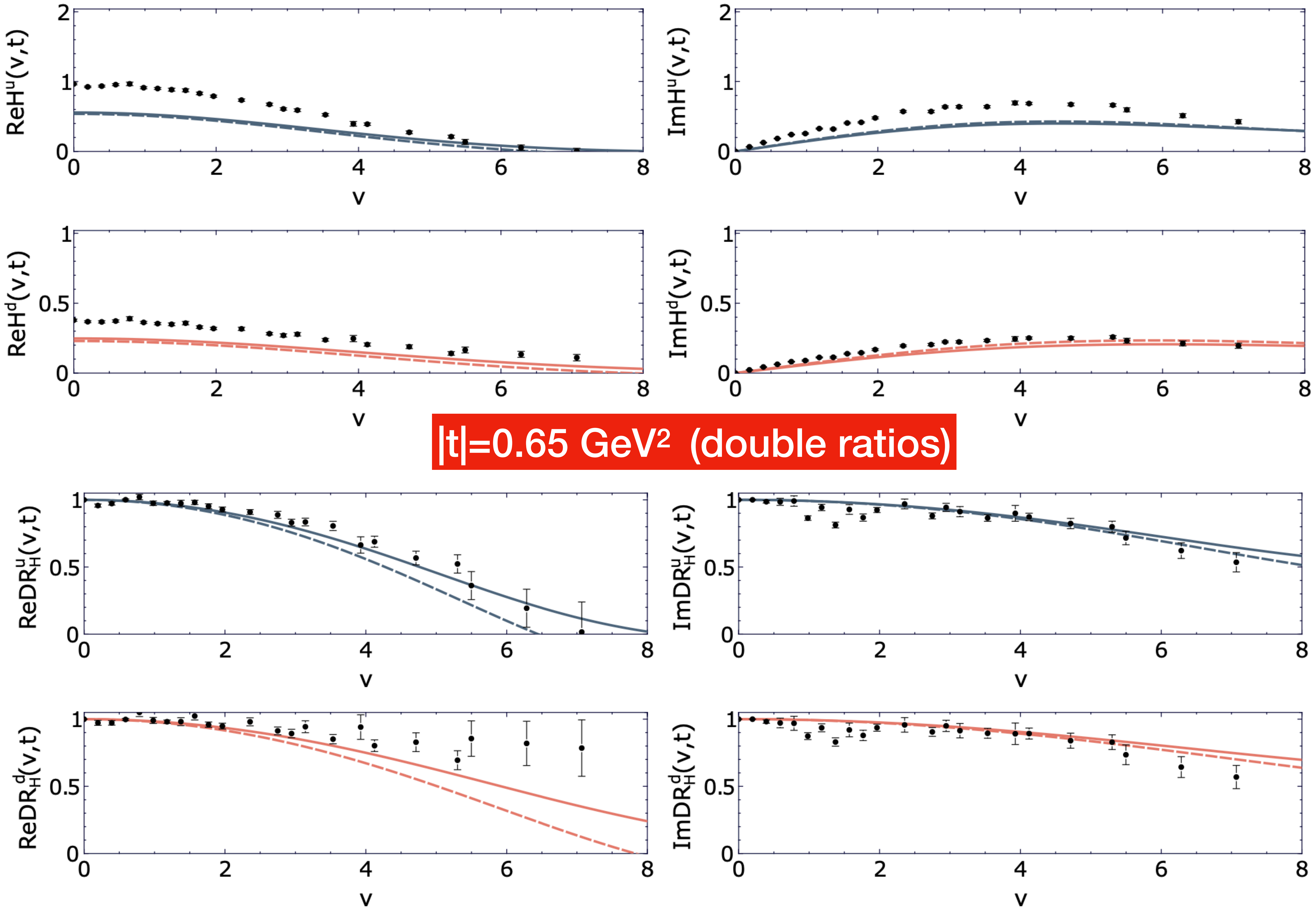

$$\mathrm{DR}_{\mathrm{Re}}(\nu, t) = \frac{\mathrm{Re}H(\nu, t)}{\mathrm{Re}H(\nu,0)} \frac{\mathrm{Re}H(0,0)}{\mathrm{Re}H(0,t)}$$

$$\mathrm{DR}_{\mathrm{Im}}(\nu, t) = \lim_{\nu'\to 0} \frac{\mathrm{Im}H(\nu, t)}{\mathrm{Im}H(\nu,0)} \frac{\mathrm{Im}H(\nu',0)}{\mathrm{Im}H(\nu', t)}$$

	up	down
GK	solid	solid
VGG	dashed	dashed

Fit to elastic and lattice-QCD data

- Fitting Ansatz for GPD H:

$$H^q(x,t) = H^q_C(x,t) + H^q_S(x,t)$$

- "classic" term

$$H^q_C(x,t) = q(x)\exp(f^q_H(x)t)$$

$$f^q_H(x) = p^q_{H,0}\log(1/x) + p^q_{H,1}(1-x)^2 - p^q_{H,0}(1-x)x$$

- "shadow" term (NEW),
  only sensitive to lattice-QCD data

$$H^q_S(x,t) = p^q_{H,2} \times \left((1-x)^{b^q_H} - A(t)(1-x)^{(b^q_H+1)}\right) \times \left(\exp(p^q_{H,3}(1-x)t) - \exp(p^q_{H,4}(1-x)t)\right)$$

- Fitting Ansatz for GPD E:

$$E^q(x,t) = e_q(x)\exp(f^q_E(x)t)$$

$$f^q_E(x) = p^q_{H,0}\log(1/x) + p^q_{E,0}(1-x)^2 + p^q_{E,1}x(1-x)$$

- Positivity enforces numerically
- We use elastic FF and lattice-QCD data (double ratios)
  → only valance quarks!
- Quality of fit: $\chi^2/\text{nPoints} \approx 1.34$

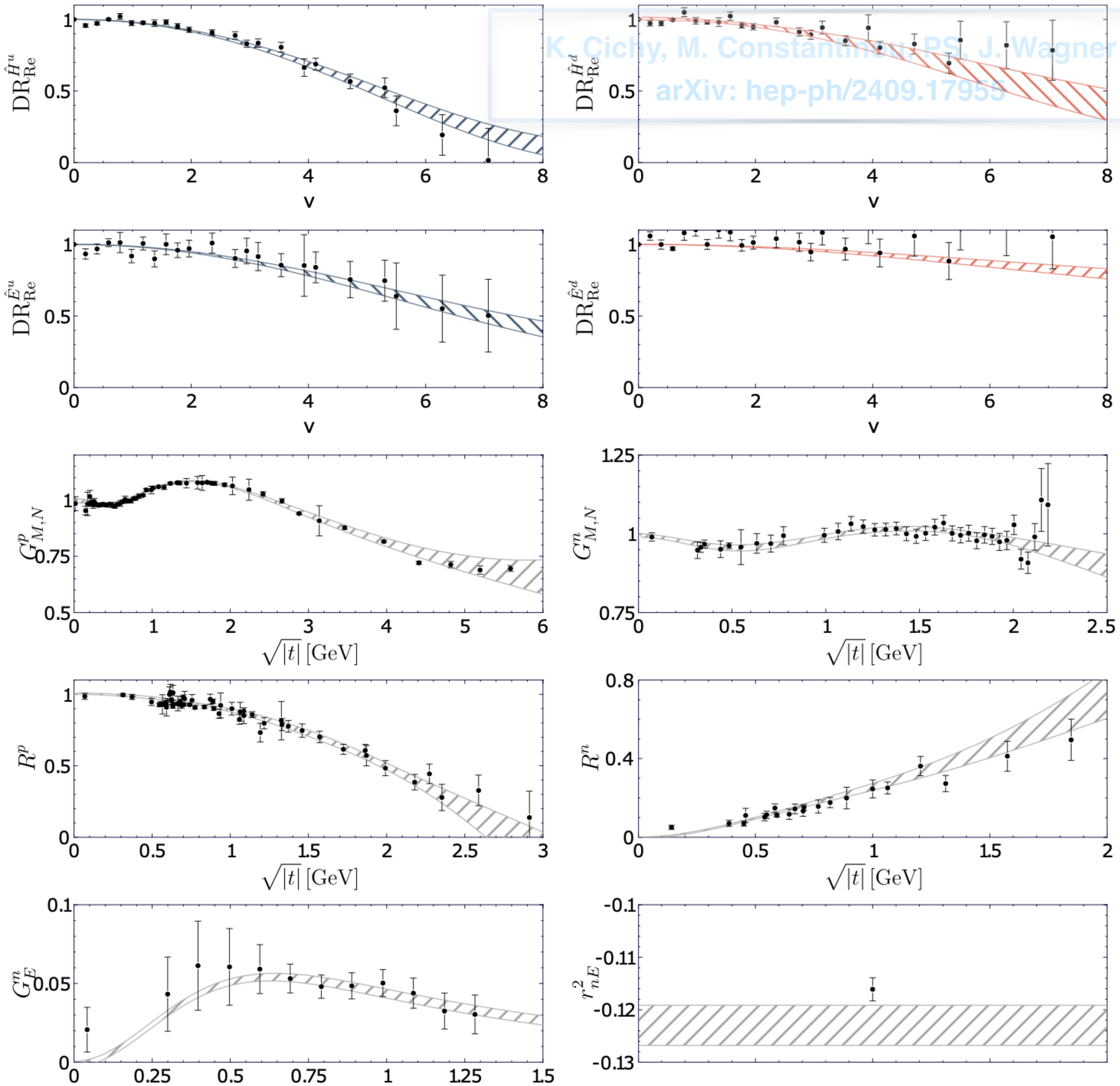

K. Cichy, M. Constantinou, PS, J. Wagner
arXiv: hep-ph/2409.17955

Results - nucleon tomography

K. Cichy, M. Constantinou, PS, J. Wagner
arXiv: hep-ph/2409.17955

x=0.2 (unpolarised proton)

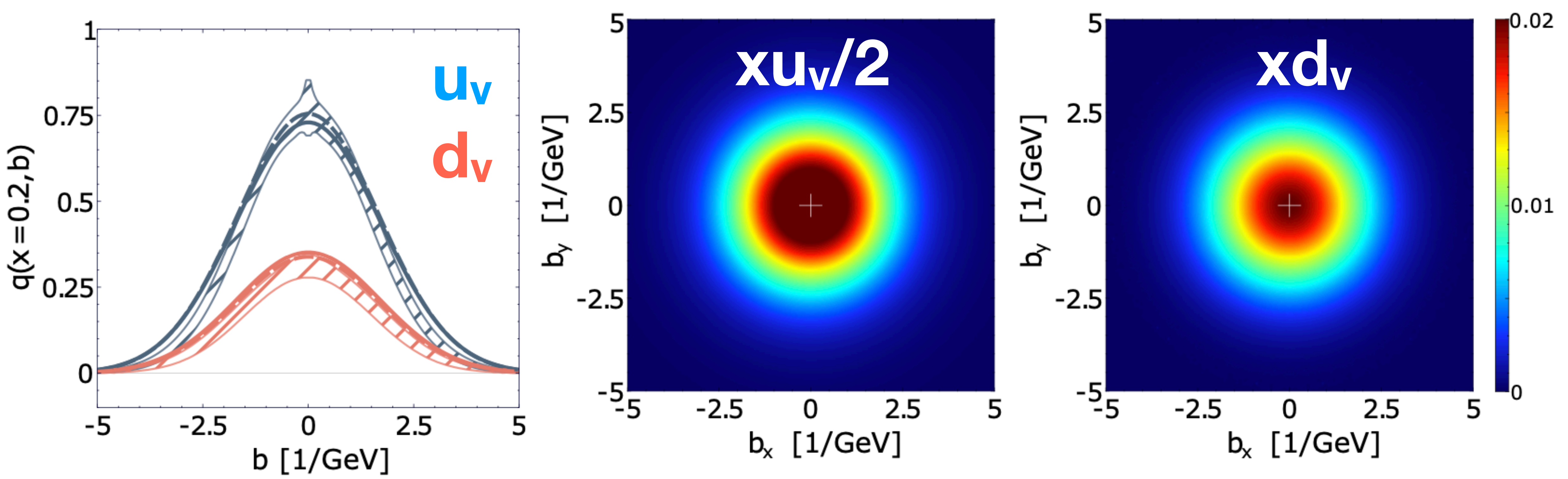

x=0.5 (unpolarised proton)

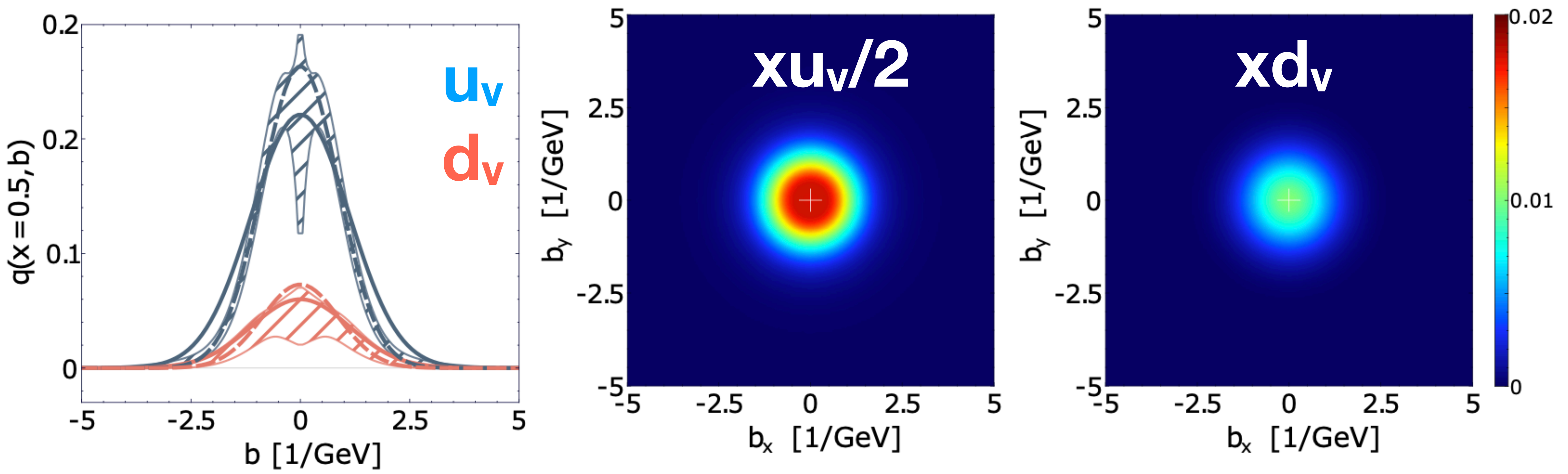

x=0.2 (transversely polarised proton)

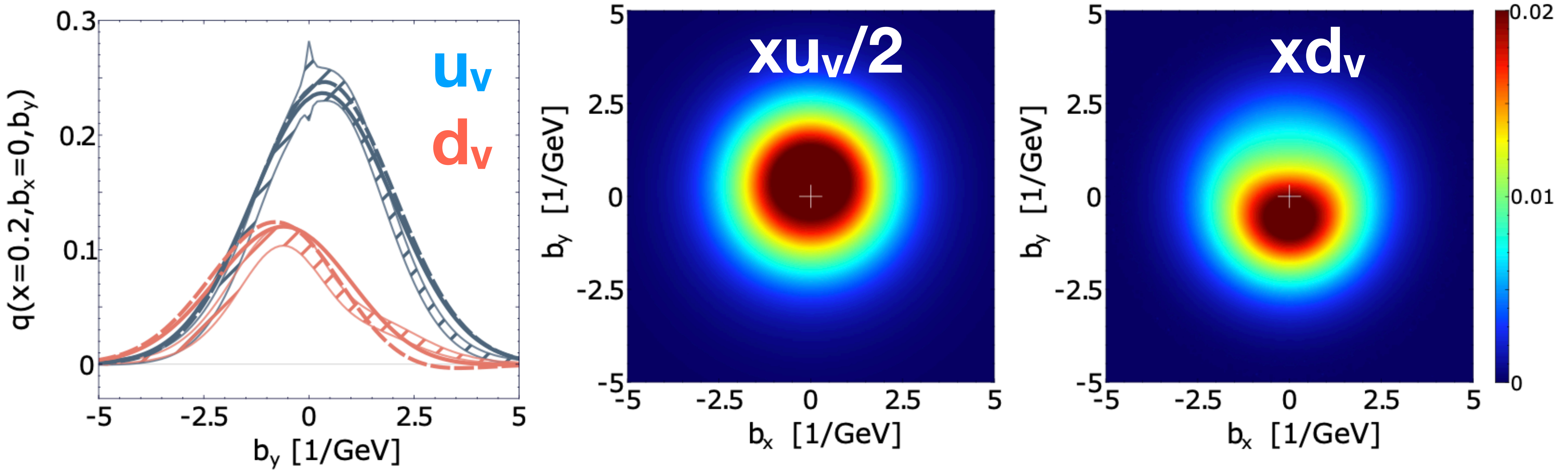

x=0.5 (transversely polarised proton)

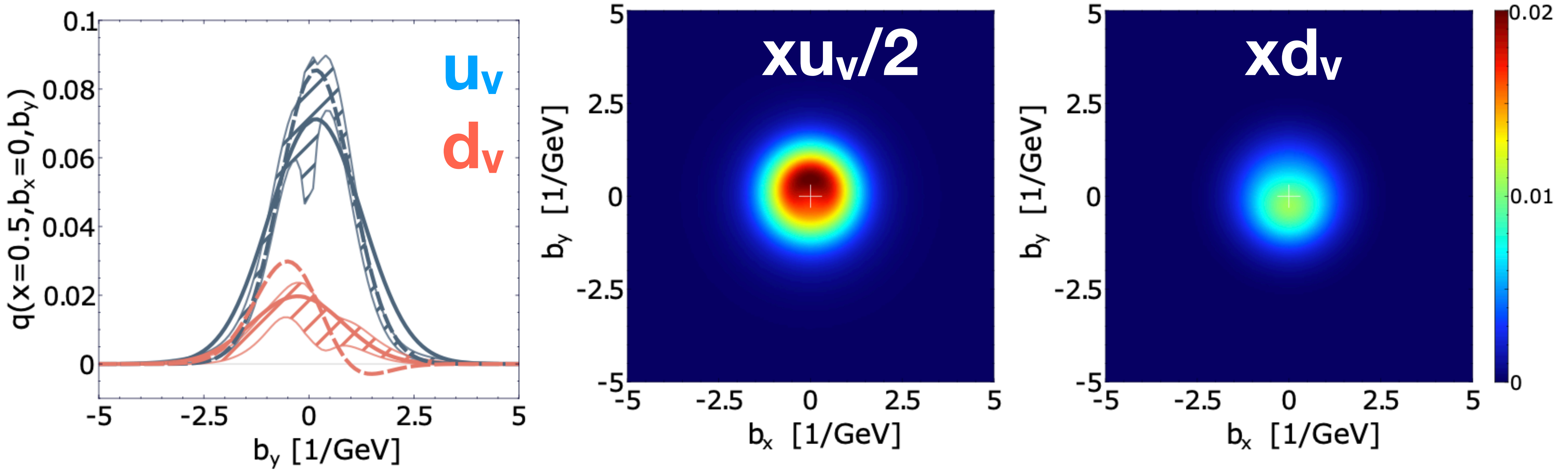

Results - total angular momentum

K. Cichy, M. Constantinou, PS, J. Wagner
arXiv: hep-ph/2409.17955

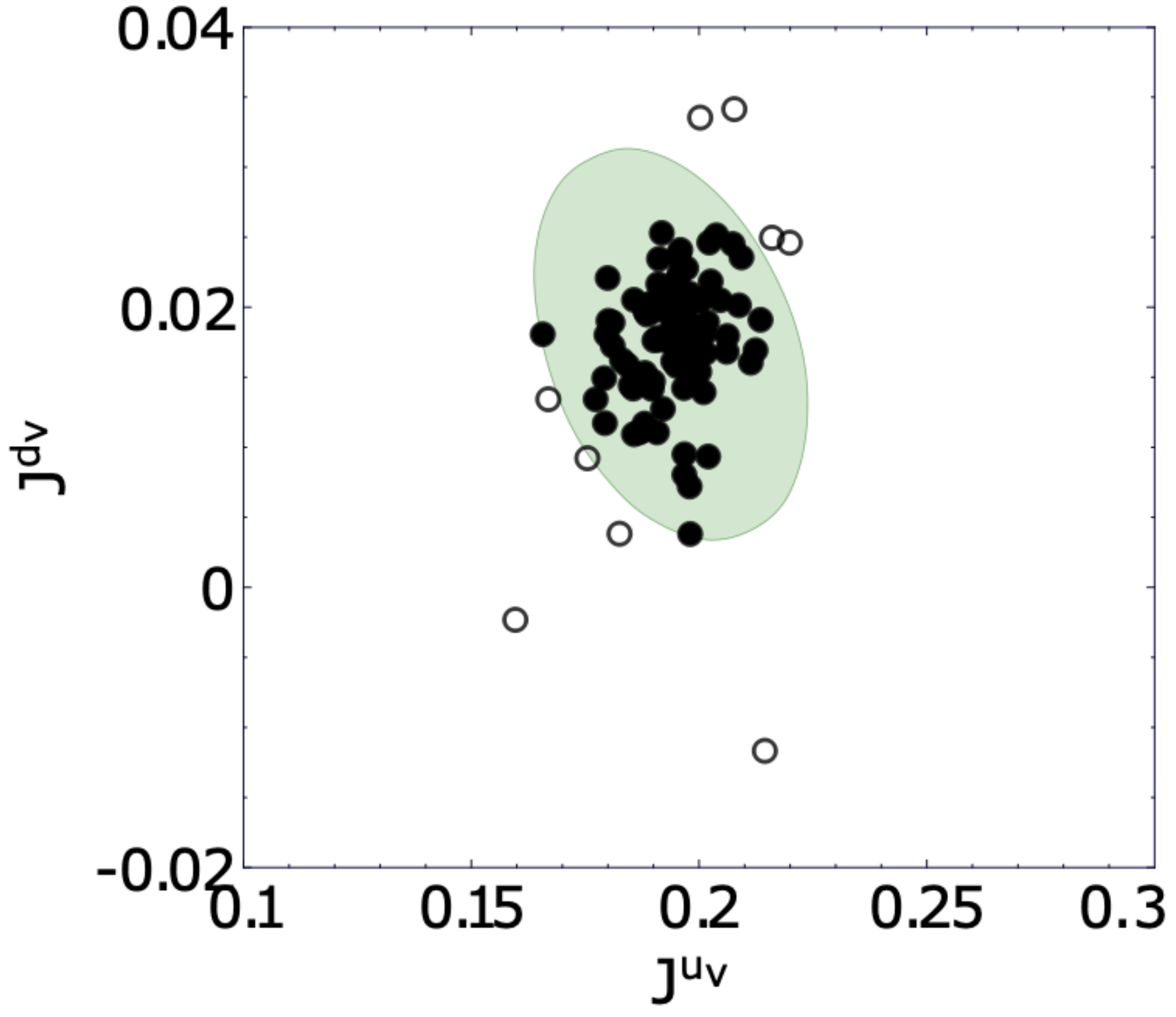

(green box)	3σ ellipse
●	replicas giving values inside ellipse
○	replicas giving values outside ellipse

Our result
(elastic and lattice-QCD data):

$$J^{u_v} = 0.195 \pm 0.010$$
$$J^{d_v} = 0.0173 \pm 0.0046$$

Diehl-Kroll / EPJC 73, 2397 (2013)
(elastic data):

$$J^{u_v} = 0.230^{+0.009}_{-0.024}$$
$$J^{d_v} = -0.004^{+0.010}_{-0.016}$$

Bacchetta-Radici / PRL 107, 212001 (2011)
(SIDIS data, Sivers function related to GPD E via Burkardt's "lensing function")

$$J^{u} = 0.229 \pm 0.002^{+0.008}_{-0.012}, \quad J^{\bar{u}} = 0.015 \pm 0.003^{+0.001}_{-0.000}$$
$$J^{d} = -0.007 \pm 0.003^{+0.020}_{-0.005}, \quad J^{\bar{d}} = 0.022 \pm 0.005^{+0.001}_{-0.000}$$

(all estimates given at μ = 2 GeV)

Summary

- Take-away messages:

  - DVCS and TCS only give limited access to GPDs,
    but still offer a wealth of important information:
    - nucleon tomography at low-xB
    - "mechanical" properties
    - Froissart-Gribov projections (now also for spin 1/2 target)

  - DDVCS allows to avoid limitations of DVCS and TCS, but is much more difficult to measure
  - new DDVCS description (including pheno. studies) available
  - new evaluation of DDVCS (and also TCS) amplitudes in terms of twist expansion will become available soon

  - new impact studies of lattice QCD data inclusion